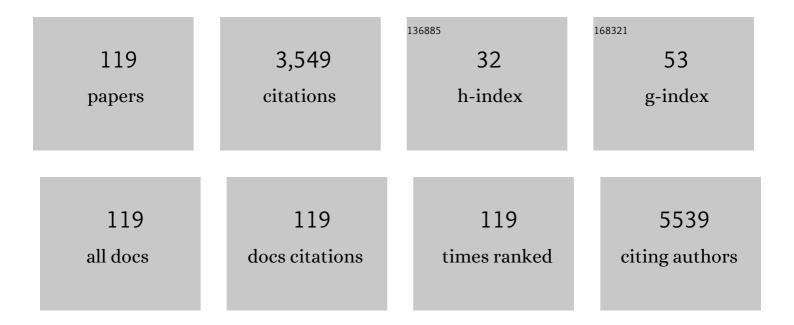
Danil Bukhvalov

List of Publications by Year in descending order

Source: https://exaly.com/author-pdf/3490080/publications.pdf Version: 2024-02-01



#	Article	IF	CITATIONS
1	Origin of Anomalous Water Permeation through Graphene Oxide Membrane. Nano Letters, 2013, 13, 3930-3935.	4.5	233
2	Metal organic frameworks as sorption media for volatile and semi-volatile organic compounds at ambient conditions. Scientific Reports, 2016, 6, 27813.	1.6	132
3	A Computational Investigation of the Catalytic Properties of Graphene Oxide: Exploring Mechanisms by using DFT Methods. ChemCatChem, 2012, 4, 1844-1849.	1.8	129
4	Triple Functions of Ni(OH) ₂ on the Surface of WN Nanowires Remarkably Promoting Electrocatalytic Activity in Full Water Splitting. ACS Catalysis, 2020, 10, 13323-13333.	5.5	120
5	Hierarchical ultrathin carbon encapsulating transition metal doped MoP electrocatalysts for efficient and pH-universal hydrogen evolution reaction. Nano Energy, 2020, 70, 104445.	8.2	118
6	The sensitive detection of formaldehyde in aqueous media using zirconium-based metal organic frameworks. Sensors and Actuators B: Chemical, 2017, 241, 938-948.	4.0	96
7	The influence of chemical reactivity of surface defects on ambient-stable InSe-based nanodevices. Nanoscale, 2016, 8, 8474-8479.	2.8	92
8	Liquidâ€Phase Exfoliated Indium–Selenide Flakes and Their Application in Hydrogen Evolution Reaction. Small, 2018, 14, e1800749.	5.2	90
9	Evidencing Interfacial Charge Transfer in 2D CdS/2D MXene Schottky Heterojunctions toward Highâ€Efficiency Photocatalytic Hydrogen Production. Solar Rrl, 2021, 5, 2000414.	3.1	83
10	Chemical modifications and stability of phosphorene with impurities: a first principles study. Physical Chemistry Chemical Physics, 2015, 17, 15209-15217.	1.3	78
11	Adsorptive removal of an eight-component volatile organic compound mixture by Cu-, Co-, and Zr-metal-organic frameworks: Experimental and theoretical studies. Chemical Engineering Journal, 2020, 397, 125391.	6.6	72
12	Tailoring the Surface Chemical Reactivity of Transitionâ€Metal Dichalcogenide PtTe ₂ Crystals. Advanced Functional Materials, 2018, 28, 1706504.	7.8	68
13	Development of Highly Water Stable Graphene Oxide-Based Composites for the Removal of Pharmaceuticals and Personal Care Products. Industrial & Engineering Chemistry Research, 2019, 58, 2899-2913.	1.8	65
14	Amine-Functionalized Metal–Organic Frameworks and Covalent Organic Polymers as Potential Sorbents for Removal of Formaldehyde in Aqueous Phase: Experimental Versus Theoretical Study. ACS Applied Materials & Interfaces, 2019, 11, 1426-1439.	4.0	65
15	Unveiling the Mechanisms Leading to H ₂ Production Promoted by Water Decomposition on Epitaxial Graphene at Room Temperature. ACS Nano, 2016, 10, 4543-4549.	7.3	60
16	Atomic structure, electronic states, and optical properties of epitaxially grown β-Ga2O3 layers. Superlattices and Microstructures, 2018, 120, 90-100.	1.4	60
17	Charge Transfer-Induced Molecular Hole Doping into Thin Film of Metal–Organic Frameworks. ACS Applied Materials & Interfaces, 2015, 7, 18501-18507.	4.0	58
18	Water Splitting over Graphene-Based Catalysts: Ab Initio Calculations. ACS Catalysis, 2014, 4, 2016-2021.	5.5	55

#	Article	IF	CITATIONS
19	Modeling of hydrogen and hydroxyl group migration on graphene. Physical Chemistry Chemical Physics, 2010, 12, 15367.	1.3	54
20	Modulation of Volmer step for efficient alkaline water splitting implemented by titanium oxide promoting surface reconstruction of cobalt carbonate hydroxide. Nano Energy, 2021, 82, 105732.	8.2	53
21	The Advent of Indium Selenide: Synthesis, Electronic Properties, Ambient Stability and Applications. Nanomaterials, 2017, 7, 372.	1.9	50
22	XPS spectra as a tool for studying photochemical and thermal degradation in APbX3 hybrid halide perovskites. Nano Energy, 2021, 79, 105421.	8.2	50
23	Unveiling the Origin of the High Catalytic Activity of Ultrathin 1T/2H MoSe ₂ Nanosheets for the Hydrogen Evolution Reaction: A Combined Experimental and Theoretical Study. ChemSusChem, 2019, 12, 5015-5022.	3.6	48
24	The characterization of Co-nanoparticles supported on graphene. RSC Advances, 2015, 5, 75600-75606.	1.7	46
25	Transitionâ€Metal Dichalcogenide NiTe ₂ : An Ambientâ€Stable Material for Catalysis and Nanoelectronics. Advanced Functional Materials, 2020, 30, 2000915.	7.8	45
26	Self-Assembled SnO ₂ /SnSe ₂ Heterostructures: A Suitable Platform for Ultrasensitive NO ₂ and H ₂ Sensing. ACS Applied Materials & Interfaces, 2020, 12, 34362-34369.	4.0	44
27	XPS and DFT study of pulsed Bi-implantation of bulk and thin-films of ZnO—The role of oxygen imperfections. Applied Surface Science, 2016, 387, 1093-1099.	3.1	41
28	Toward the Effective Exploitation of Topological Phases of Matter in Catalysis: Chemical Reactions at the Surfaces of NbAs and TaAs Weyl Semimetals. Advanced Functional Materials, 2018, 28, 1800511.	7.8	40
29	Anisotropic magnetism of graphite irradiated with medium-energy hydrogen and helium ions. Physical Review B, 2011, 83, .	1.1	39
30	The atomic and electronic structure of nitrogen- and boron-doped phosphorene. Physical Chemistry Chemical Physics, 2015, 17, 27210-27216.	1.3	38
31	Structural phase transitions in VSe ₂ : energetics, electronic structure and magnetism. Physical Chemistry Chemical Physics, 2019, 21, 22647-22653.	1.3	37
32	Sn-loss effect in a Sn-implanted a-SiO2 host-matrix after thermal annealing: A combined XPS, PL, and DFT study. Applied Surface Science, 2016, 367, 320-326.	3.1	35
33	xmlns:mml="http://www.w3.org/1998/Math/Math/MathML" display="inline"> < mml:mrow> < mml:mi> p < /mml:mi> < mml:mo> â^' < /mml:mo> < mml:mi> p < /mml:mrow> in carbon-doped In < mml:math xmlns:mml="http://www.w3.org/1998/Math/MathML" display="inline"> < mml:msub> < mml:mrow	1.1	nth>coupling 33
34	Formation of a Quasiâ€Freeâ€Standing Single Layer of Graphene and Hexagonal Boron Nitride on Pt(111) by a Single Molecular Precursor. Advanced Functional Materials, 2016, 26, 1120-1126.	7.8	33
35	A new triboelectric nanogenerator with excellent electric breakdown self-healing performance. Nano Energy, 2021, 85, 105990.	8.2	33
36	The role of surface chemical reactivity in the stability of electronic nanodevices based on two-dimensional materials "beyond graphene―and topological insulators. FlatChem, 2017, 1, 60-64.	2.8	32

#	Article	IF	CITATIONS
37	Atomic and electronic structures of stable linear carbon chains on Ag-nanoparticles. Carbon, 2018, 128, 296-301.	5.4	32
38	Switching the Nonlinear Optical Absorption of Titanium Carbide MXene by Modulation of the Surface Terminations. ACS Nano, 2022, 16, 394-404.	7.3	32
39	Metal–Organic Frameworks for the Adsorptive Removal of Gaseous Aliphatic Ketones. ACS Applied Materials & Interfaces, 2020, 12, 10317-10331.	4.0	31
40	Molecular dynamics simulation insight into the temperature dependence and healing mechanism of an intrinsic self-healing polyurethane elastomer. Physical Chemistry Chemical Physics, 2020, 22, 17620-17631.	1.3	30
41	Electronic structure of magnetic moleculesV15:â€,â€,LSDA+U calculations, x-ray emissions, and photoelectron spectra. Physical Review B, 2003, 67, .	1.1	29
42	Ligand-Controlled Magnetic Interactions in Mn4 Clusters. Inorganic Chemistry, 2009, 48, 11903-11908.	1.9	28
43	Modeling of epitaxial graphene functionalization. Nanotechnology, 2011, 22, 055708.	1.3	28
44	XPS and DFT study of Sn incorporation into ZnO and TiO ₂ host matrices by pulsed ion implantation. Physica Status Solidi (B): Basic Research, 2015, 252, 1890-1896.	0.7	28
45	The MRO-accompanied modes of Re-implantation into SiO2-host matrix: XPS and DFT based scenarios. Journal of Alloys and Compounds, 2017, 728, 759-766.	2.8	28
46	Effect of Ligand Substitution on the Exchange Interactions in {Mn ₁₂ }-Type Single-Molecule Magnets. Inorganic Chemistry, 2010, 49, 10902-10906.	1.9	27
47	PdTe ₂ Transitionâ€Metal Dichalcogenide: Chemical Reactivity, Thermal Stability, and Device Implementation. Advanced Functional Materials, 2020, 30, 1906556.	7.8	27
48	Hydrogen Dissociation Catalyzed by Carbon oated Nickel Nanoparticles: Experiment and Theory. ChemPhysChem, 2013, 14, 381-385.	1.0	26
49	Study of the Structural Characteristics of 3d Metals Cr, Mn, Fe, Co, Ni, and Cu Implanted in ZnO and TiO ₂ —Experiment and Theory. Journal of Physical Chemistry C, 2014, 118, 28143-28151.	1.5	26
50	Unveiling the origin of room-temperature ferromagnetism in monolayer VSe2: the role of extrinsic effects. Nanoscale, 2020, 12, 20875-20882.	2.8	26
51	Utilization of metal–organic frameworks for the adsorptive removal of an aliphatic aldehyde mixture in the gas phase. Nanoscale, 2020, 12, 8330-8343.	2.8	25
52	Cellulose Hydrogels by Reversible Ionâ€Exchange as Flexible Pressure Sensors. Advanced Materials Technologies, 2020, 5, 2000358.	3.0	25
53	Application of Zr-Cluster-Based MOFs for the Adsorptive Removal of Aliphatic Aldehydes (C ₁ to C ₅) from an Industrial Solvent. ACS Applied Materials & Interfaces, 2019, 11, 44270-44281.	4.0	23
54	Charge Redistribution Mechanisms in SnSe ₂ Surfaces Exposed to Oxidative and Humid Environments and Their Related Influence on Chemical Sensing. Journal of Physical Chemistry Letters, 2020, 11, 9003-9011.	2.1	23

#	Article	IF	CITATIONS
55	Bi-doped silica glass: A combined XPS – DFT study of electronic structure and pleomorphic imperfections. Journal of Alloys and Compounds, 2020, 829, 154459.	2.8	23
56	Reactive adsorption and catalytic oxidation of gaseous formaldehyde at room temperature by a synergistic copper-magnesium bimetal oxide biochar composite. Chemical Engineering Journal, 2022, 433, 133497.	6.6	22
57	NiSe and CoSe Topological Nodalâ€Line Semimetals: A Sustainable Platform for Efficient Thermoplasmonics and Solarâ€Driven Photothermal Membrane Distillation. Small, 2022, 18, .	5.2	21
58	Modification of titanium and titanium dioxide surfaces by ion implantation: Combined XPS and DFT study. Physica Status Solidi (B): Basic Research, 2015, 252, 748-754.	0.7	20
59	Octahedral conversion of a-SiO ₂ host matrix by pulsed ion implantation. Physica Status Solidi (B): Basic Research, 2015, 252, 2185-2190.	0.7	19
60	H-bond/ionic coordination switching for fabrication of highly oriented cellulose hydrogels. Journal of Materials Chemistry A, 2021, 9, 5533-5541.	5.2	19
61	Novel Molecular-Level Insight into the Self-Healing Behavior and Mechanism of Polyurethane-Urea Elastomer Based on a Noncovalent Strategy. Macromolecules, 2022, 55, 4776-4789.	2.2	19
62	Amine-functionalized microporous covalent organic polymers for adsorptive removal of a gaseous aliphatic aldehyde mixture. Environmental Science: Nano, 2020, 7, 3447-3468.	2.2	18
63	Influence of Ion Migration from ITO and SiO ₂ Substrates on Photo and Thermal Stability of CH ₃ NH ₃ SnI ₃ Hybrid Perovskite. Journal of Physical Chemistry C, 2020, 124, 14928-14934.	1.5	18
64	Firstâ€principles modeling of the interactions of iron impurities with graphene and graphite. Physica Status Solidi (B): Basic Research, 2011, 248, 1347-1351.	0.7	16
65	Unusually strong lateral interaction in the CO overlayer in phosphorene-based systems. Nano Research, 2016, 9, 2598-2605.	5.8	15
66	Understanding Mechanism of Adsorption in the Decolorization of Aqueous Methyl Violet (6B) Solution by Okra Polysaccharides: Experiment and Theory. ACS Omega, 2019, 4, 17880-17889.	1.6	15
67	Interaction of graphene oxide with barium titanate in composite: XPS and DFT studies. Journal of Alloys and Compounds, 2020, 840, 155747.	2.8	15
68	Development of Theoretical Descriptors for Cytotoxicity Evaluation of Metallic Nanoparticles. Chemical Research in Toxicology, 2017, 30, 1549-1555.	1.7	14
69	Efficient hydrogen evolution reaction with platinum stannide PtSn ₄ <i>via</i> surface oxidation. Journal of Materials Chemistry A, 2020, 8, 2349-2355.	5.2	14
70	Thermal Effects and Halide Mixing of Hybrid Perovskites: MD and XPS Studies. Journal of Physical Chemistry A, 2020, 124, 135-140.	1.1	14
71	Structural defects and electronic structure of N-ion implanted TiO 2 : Bulk versus thin film. Applied Surface Science, 2015, 355, 984-988.	3.1	13
72	Chemical reactions on surfaces for applications in catalysis, gas sensing, adsorption-assisted desalination and Li-ion batteries: opportunities and challenges for surface science. Physical Chemistry Chemical Physics, 2021, 23, 7541-7552.	1.3	13

#	Article	IF	CITATIONS
73	Enhancing Reverse Saturable Absorption in SnS ₂ Nanosheets by Plasma Treatment. ACS Applied Materials & Interfaces, 2021, 13, 4211-4219.	4.0	13
74	Mitrofanovite Pt ₃ Te ₄ : A Topological Metal with Termination-Dependent Surface Band Structure and Strong Spin Polarization. ACS Nano, 2021, 15, 14786-14793.	7.3	13
75	Unveiling the Mechanisms Ruling the Efficient Hydrogen Evolution Reaction with Mitrofanovite Pt ₃ Te ₄ . Journal of Physical Chemistry Letters, 2021, 12, 8627-8636.	2.1	13
76	Bulk In2O3 crystals grown by chemical vapour transport: a combination of XPS and DFT studies. Journal of Materials Science: Materials in Electronics, 2019, 30, 18753-18758.	1.1	12
77	Low-temperature oxidative removal of gaseous formaldehyde by an eggshell waste supported silver-manganese dioxide bimetallic catalyst with ultralow noble metal content. Journal of Hazardous Materials, 2022, 434, 128857.	6.5	12
78	Atomic, electronic and magnetic structure of graphene/iron and nickel interfaces: theory and experiment. RSC Advances, 2015, 5, 9173-9179.	1.7	11
79	Absence of a stable atomic structure in fluorinated graphene. Physical Chemistry Chemical Physics, 2016, 18, 13287-13293.	1.3	11
80	Hybrid Surface Passivation for Retrieving Charge Collection Efficiency of Colloidal Quantum Dot Photovoltaics. ACS Applied Materials & Interfaces, 2020, 12, 43576-43585.	4.0	11
81	Tin Diselenide (SnSe2) Van der Waals Semiconductor: Surface Chemical Reactivity, Ambient Stability, Chemical and Optical Sensors. Materials, 2022, 15, 1154.	1.3	11
82	Bulk vs. Surface Structure of 3d Metal Impurities in Topological Insulator Bi2Te3. Scientific Reports, 2017, 7, 5758.	1.6	10
83	Atomic and electronic structure of graphene oxide/Cu interface. Thin Solid Films, 2018, 665, 99-108.	0.8	10
84	Under-cover stabilization and reactivity of a dense carbon monoxide layer on Pt(111). Chemical Science, 2019, 10, 1857-1865.	3.7	10
85	Local atomic configurations, energy structure, and optical properties of implantation defects in Gd-doped silica glass: An XPS, PL, and DFT study. Journal of Alloys and Compounds, 2019, 796, 77-85.	2.8	10
86	First-principle studies of optical properties of Be Zn1-O ternary mixed crystal. Optik, 2019, 178, 691-697.	1.4	10
87	Interaction of VSe ₂ with Ambient Gases: Stability and Chemical Reactivity. Physica Status Solidi - Rapid Research Letters, 2020, 14, 1900332.	1.2	10
88	Effect of long-term storage on the electronic structure of semiconducting silicon wafers implanted by rhenium ions. Journal of Materials Science, 2021, 56, 2103-2112.	1.7	10
89	Terahertz Photodetection with Typeâ€l Dirac Fermions in Transitionâ€Metal Ditellurides and Their Heterostructures. Physica Status Solidi - Rapid Research Letters, 2021, 15, 2100212.	1.2	10
90	Formation of Fe–Fe Antiferromagnetic Dimers in Doped TiO2:Fe Nanoparticles. Journal of Physical Chemistry C, 2019, 123, 1494-1505.	1.5	9

#	Article	IF	CITATIONS
91	Efficient Electrochemical Water Splitting with PdSn ₄ Dirac Nodal Arc Semimetal. ACS Catalysis, 2021, 11, 7311-7318.	5.5	9
92	Synthesis and Magnetic Properties of Mn12-Based Single Molecular Magnets with Benzene and Pentafluorobenzene Carboxylate Ligands. Journal of Superconductivity and Novel Magnetism, 2011, 24, 855-859.	0.8	8
93	Effect of doping and annealing on the electronic structure and magnetic properties of nanoscale Co and Zn co-doped SnO2: An experimental study and first-principles modeling. Journal of Alloys and Compounds, 2019, 799, 433-441.	2.8	8
94	Unconventional magnetism of non-uniform distribution of Co in TiO2 nanoparticles. Journal of Alloys and Compounds, 2020, 826, 154194.	2.8	8
95	Kitkaite NiTeSe, an Ambient‣table Layered Dirac Semimetal with Lowâ€Energy Typeâ€II Fermions with Application Capabilities in Spintronics and Optoelectronics. Advanced Functional Materials, 0, , 2106101.	7.8	8
96	Quality assessment of GaN epitaxial films: Acidification scenarios based on XPS-and-DFT combined study. Applied Surface Science, 2021, 563, 150308.	3.1	8
97	Computational calculation identified optimal binding sites in nano-sized magnetic-cored dendrimer. Chemosphere, 2018, 210, 287-295.	4.2	7
98	Noncovalent bonding of copper atoms to the nitrogen-containing sites of hydrogenated diamond surfaces. Mendeleev Communications, 2019, 29, 452-454.	0.6	7
99	III–VI and IV–VI van der Waals Semiconductors InSe, GaSe and GeSe: A Suitable Platform for Efficient Electrochemical Water Splitting, Photocatalysis and Chemical Sensing. Israel Journal of Chemistry, 2022, 62, .	1.0	7
100	Surface Instability and Chemical Reactivity of ZrSiS and ZrSiSe Nodal‣ine Semimetals. Advanced Functional Materials, 2019, 29, 1900438.	7.8	6
101	Chemical instability of free-standing boron monolayers and properties of oxidized borophene sheets. Physica E: Low-Dimensional Systems and Nanostructures, 2020, 120, 114082.	1.3	6
102	TiO ₂ -enhanced <i>in situ</i> electrochemical activation of Co ₃ O ₄ for the alkaline hydrogen evolution reaction. Journal of Materials Chemistry A, 2022, 10, 13769-13779.	5.2	6
103	Enhanced clustering tendency of Cu-impurities with a number of oxygen vacancies in heavy carbon-loaded TiO2 - the bulk and surface morphologies. Solid State Sciences, 2017, 71, 130-138.	1.5	5
104	Catalytic activity of PtSn4: Insights from surface-science spectroscopies. Applied Surface Science, 2020, 514, 145925.	3.1	5
105	A new aggregation induced emission enhancement (AIEE) dye which self-assembles to panchromatic fluorescent flowers and has application in sensing dichromate ions. Soft Matter, 2022, 18, 3019-3030.	1.2	5
106	X-ray photoelectron spectra and electronic structure of Mo doped V2O5. Thin Solid Films, 2020, 713, 138360.	0.8	4
107	Long range interactions and related carbon–carbon bond reconstruction between interior and surface defects in nanodiamonds. Physical Chemistry Chemical Physics, 2021, 23, 14592-14600.	1.3	3
108	Unveiling the Atomic and Electronic Structure of Stacked-Cup Carbon Nanofibers. Nanoscale Research Letters, 2021, 16, 153.	3.1	3

#	Article	IF	CITATIONS
109	Efficient Hydrogen Evolution Reaction with Bulk and Nanostructured Mitrofanovite Pt3Te4. Nanomaterials, 2022, 12, 558.	1.9	3
110	Sequestration of carbon monoxide at room temperature at vacancy sites of graphene. Chemical Communications, 2019, 55, 8607-8610.	2.2	2
111	On the atomic structure of two-dimensional materials with Janus structures. Physical Chemistry Chemical Physics, 2022, 24, 9836-9841.	1.3	2
112	Electronic structure and structural defects in 3d-metal doped In2O3. Journal of Materials Science: Materials in Electronics, 2019, 30, 14091-14098.	1.1	1
113	First-Principles Modeling of Atomic Structure and Chemical and Optical Properties of β-C3N4. Journal of Carbon Research, 2019, 5, 58.	1.4	1
114	Fabrication of Conjugated Porous Polymer Catalysts for Oxygen Reduction Reactions: A Bottom-Up Approach. Catalysts, 2020, 10, 1224.	1.6	1
115	Structure and Magnetic Properties of Superoxide Radical Anion Complexes with Low Binding Energy at the Graphene Edges. Russian Journal of Coordination Chemistry/Koordinatsionnaya Khimiya, 2020, 46, 738-745.	0.3	1
116	Engineering ferromagnetic lines in graphene by local oxidation and hydrogenation using nanoscale lithography. Journal Physics D: Applied Physics, 2021, 54, 074002.	1.3	1
117	Effect of vacancy defects on electronic structure and ferromagnetism in pristine In2O3 nanostructures: An experimental study and first-principles modeling. Materials Research Bulletin, 2022, 152, 111853.	2.7	1
118	Modeling of electronic and optical properties of C3N4 within DFT frame. AIP Conference Proceedings, 2019, , .	0.3	0
119	Uncommon clustering in dilute Ti–Fe alloys. JPhys Materials, 2020, 3, 025007.	1.8	0